Journal of Manufacturing Engineering, March 2023, Vol. 18, Issue. 1, pp 030-036

DEFECT SIZE CHARACTERIZATION IN UNIDIRECTIONAL CURVED GFRP COMPOSITE BY TSR PROCESSED PULSE AND LOCK IN THERMOGRAPHY: A COMPARISON STUDY

***Gomathi R[1] and Ramkumar K[2]**

[1]Department of Physics, V.S.B. College of Engineering Technical Campus, Coimbatore, Tamil Nadu- 642 109, India
[2]Department of Quality Control, Bharat Earth Movers Limited, Palakkad, Kerala-678 621, India

ABSTRACT

Glass fiber reinforced polymer (GFRP) curved composite is widely used in industries due to its high corrosive resistance nature. GFRP curved composites are involved in many industries like petrochemical industries for handling oil and gas at offshore platforms, chemical processes such as chemical storage tanks, desalination, and water treatment. Since alloy steel materials get corroded by environmental factors such as excess salinity in the surrounding environment, mud deposition, and sulfur crude accumulation makes alloy steel pipes are expensive to maintain. Every year billions of dollars can be saved by corrosion prevention using Glass Fiber Reinforced Polymer (GFRP) pipes instead of alloy steel pipes. In-service stage of the GFRP pipe or tank, different types of defects are forming such as void, delamination, and wall loss (pits). Among all these defects, pits or wall loss is one of the severe defects which may lead to leakage accidents. The objective of the study is the quantification of defect size by using TSR processed pulsed and lock-in thermography and analyses their capabilities in defect size quantification. TSR processed the PT image and the signal to noise ratio was used to estimate the defect size quantification. For defect size measurement, the TSR-processed PT thermal results are recommended and the near-surface defects can be measured with high accuracy in LT.

.

Keywords: *Glass-fiber reinforced polymer pipe; Pulsed thermography;Lock-in thermography; Defect size; Aspect Ratio*

1. Introduction

Infrared thermography (IRT) is one of the advanced non-destructive testing methods. The advantages include large area coverage of inspection with non-contact mode and fast inspection rates [Bates et al. 2000]. In active thermography, PT and LT are major NDE techniques. These techniques are widely used in material characterization, defect detection, and quantification of composites [Sharath et al. 2012; Vijayaraghavan et al. 2011].

Pulsed thermography is used to measure the thermal properties like thermal conductivity and thermal diffusivity of different materials. At the initial stage, PT was used to defect detection (qualitative tool) and later it has been using for defect quantification. It is used to defect detection and quantification in different engineering materials such as composites and metals. Infrared Thermography is a valid tool for an estimate the fatigue behavior of GFRP composites [Colombo et al. 2011]. Moskovchenko et al. [2020] carried out delamination detection in GFRP composite using pulsed thermography and the efficiency of the Xenon flash tube and laser IR thermography has been compared. Pulsed thermography is a simple and fast investigation method for impact damage assessment of GFRP composite [Ghiseok et al. 2015]. Thermographic Signal Reconstructed (TSR) first and second derivative images of GFRP composites are enhanced the defect detectability for smaller and deeper defects [Quek and Almond 2005].

Lock-in thermography was developed by G. Busse and Karpen [1992] when the test specimen is heated using halogen lamps, and the temperature modulation caused by periodic input optical heat is recorded using an IR camera. Then a Four Point Correlation method is used to obtain the phase and amplitude information at each pixel. The authors have used this method for finding delamination in Carbon Fiber Reinforced Plastic (CFRP) composite. Infrared thermography is one of the well-known NDE methods to detect surface and subsurface defects in metals, polymers, and composite materials [Olga Wysocka-Fotek, et al. 2012; Sharath et al.2015]. Lock-in thermal NDE technique makes use of periodic optical stimulation to heat the sample, using sinusoidally

**Corresponding Author - E- mail: gggomathi@gmail.com*

modulated halogen lamps. In the technique, as proposed by Busse [1979], a continuous modulated light source is used to heat the sample and the thermal waves propagate inside the material due to conduction and interference. Lock-in thermal NDE technique can provide quantitative information on defect location, size, and depth in metals and composites [Montanini, R, 2010; Menaka et al. 2009; Choia et al. 2008; Sharath et al. 2015; Ranjith, S et al. 2016]. Sakagami et al. [2002] experimentally studied the lock-in IR application on stainless steel and reported that phase and amplitude thermal images gave significant contrast changes for crack tip detection.

Glass fiber reinforced polymer (GFRP) curved composites are widely used in industries due to their high corrosive resistance nature. GFRP curved composites are used in many industries like petrochemical industries for handling oil and gas at offshore platforms, chemical processes such as chemical storage tanks, desalination, and water treatment. Since alloy steel materials get corroded by environmental factors such as excess salinity in the surrounding environment, mud deposition, and sulfur crude accumulation makes alloy steel pipes are expensive to maintain. Every year billions of dollars can be saved by corrosion prevention using Glass Fiber Reinforced Polymer (GFRP) pipes instead of alloy steel pipes [Hassen et al. 2015]. At low temperature and pressure applications, GFRP is a good alternative for conventional alloy steel. The advantages of these FRP pipelines also include being lightweight, having few workers sufficient to install thousands of meters of the pipeline, having long service life, and low maintenance cost.

The damages in aircraft composite structures of GFRP and CFRP have been studied by Infrared thermography and small defects are not able to detect in GFRP [Andrzej Katunin et al.]. The artificial defects were characterised in AISI austenitic steel using Infrared thermography and found good results [Sharath et al.]. Andreas Kromik et al. have studied unidirectional and cross ply laminate composites and analysed the results quantitatively. They have found, the shape of the defects is clearly affected by anisotropy.

In-service stage of the GFRP pipe or tank, different types of defects are forming such as void, delamination, and wall loss (pits). Among all these defects pits or wall loss is one of the severe defects which may lead to leakage accidents [Vijayaraghavan et al. 2011]. Gomathi et al. studied defect size and depth quantification in GFRP using PT and LT thermography. They found that the measurement of the defect's depth with high accuracy in both of the techniques (PT & LT). Defect detection capabilities are compared with Pulsed and lock-in thermography using equal excitation energy and signal- to-noise ratio was also analyzed [Simon Pickering et. al. 2008, Krishnendu Chatterjee et al. 2011]. This study investigates the quantification of defect size by using pulsed and lock-in thermography and analyzes their capabilities in defect size quantification. For defect sizing Full width at half maximum has been used [Saintey et al.1995].

Signal-to-noise ratio is compared between two cameras cooled focal plane array infrared camera and an un-cooled microbolometer array camera and found that the cooled FPA infrared camera exhibits a higher ultimate defect detection capability than the un-cooled microbolometer array camera [S. G. Pickering et al. 2007]. There are different thermal image processing techniques such as independent component analysis (ICA) and Principle component thermography (PCT) used for analyzing small and deep defects [Julien R.Fleuret et al. 2021]. Yoonjae Chung et al. [2020] analyzed the material thinning due to wall loss in steel plates it was analyzed by three different signal processing methods of thermography called thermographic signal reconstruction (TSR), Principle component thermography (PCT), and pulsed phase thermography (PPT). Thermographic Signal Reconstructed (TSR) first and second derivative images of GFRP composites are enhanced the defect detectability for smaller and deeper defects [Quek and Almond 2005]. In this study, TSR processed results have been used for defect size in pulsed thermography.

2. Theory

2.1 Pulsed Thermography

IR thermography is a real-time and non-contact technique. Pulsed transient thermography is the most widely used NDT and E technique [25-27]. In PT short and high-energy pulse of light energy impinges on the sample surface. The front surface thermal energy penetrates inside the test sample due to conduction. If any interface such as voids and inclusion is present inside the sample it affects the temperature flow. Based on the defect type and size, thermal energy reflects the sample surface and an IR camera is used to capture these thermal images.

The rate of variation of temperature on the surface depends on the defect depth given by,

$$T(0,t) = \left(\frac{Q}{\sqrt{\pi \rho c k t}} \right) \left[1 + 2 \sum_{n=1}^{\infty} R^n \exp\left(\frac{-n^2 L^2}{\alpha t} \right) \right] \quad (1)$$

Where T is surface temperature, Q is the incident heat flux, **ρ** is the test material density, c is specific heat, L specimen thickness, t is time, α is thermal diffusivity of the material and n is the number of reverberations.

2.1.1 TSR processed pulsed thermography

The thermographic signal reconstruction (TSR) process removes noise from the defect signal and improves signal-to-noise of PT results [30-31]. A comparison of TSR with conventional thermographic approaches shows that the performance improvements of TSR results [32]. Signal–to-background contrast is significantly increased when images are based on the time derivatives of the TSR signal. In this study, TSR processed pulsed first derivative image is used to estimate the defect size.

In this study, an unprocessed PT image is converted to ASCII code and this code is fitted for 7th order polynomial using TSR coding. Then the reconstructed first derivative image of processed TSR is taken for further analysis.

2.2 Lock-In Thermography

Lock-in thermography is one of the most commonly accepted NDT techniques [28-29]. In lock-in thermography, the testing sample is heated by periodical thermal wave use of modulated heat source. The thermal wave which falls on the surface propagates inside the material. When this thermal wave met the internal defects such as voids, delamination, wall loss, etc., it reflected the surface and interacted with an incoming thermal wave. The resulting modified modulated surface thermal wave was captured by an IR camera. Four equidistant points (I1, I2, I3 & I4) correlation is performed on each pixel on the image. Then amplitude (A) and phase (Ø) values at each pixel can be computed using the following equations [2 & 3].

$$A(z) = \frac{1}{2}\sqrt{(I_3 - I_1)^2 + (I_4 - I_2)^2} \qquad (2)$$

$$\phi(Z) = \left(\frac{I_3 - I_1}{I_4 - I_2}\right) \qquad (3)$$

In this study, we considered phase images for defect size quantification.

3. Sample Preparation

Filament wounding unidirectional E glass epoxy adhesive pipe dimension of 164 mm outer diameter and 6 mm thickness with a glass content of 76% by weight was manufactured. The fiber orientation angle was 54°. The Schematic diagram of the fabricated sample is shown in figure 1. To study the defect size quantification artificially created flat bottom holes of 6 mm diameter at depth of 0.6mm, 1.2mm, 1.8mm, 2.4mm, 3.00mm, 3.6mm, and 4.2mm from the outer wall of the GFRP curved composite pipe (Fig.1). The flat bottom holes were fabricated in GFRP using a CNC machine with an end mill cutter. These flat bottom holes are used for defect size quantification using both TSR processed PT and LT. A uniform thin black coating is applied on the sample's surface to overcome the emissivity problems.

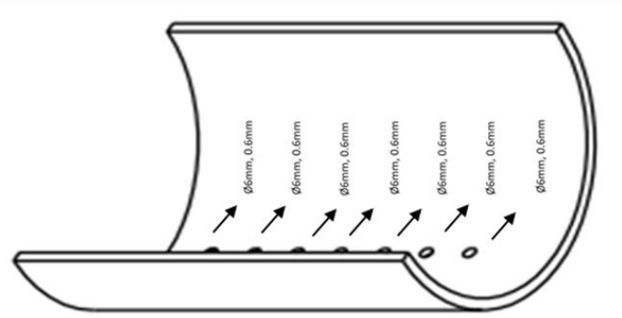

Fig. 1 Representation of a GFRP sample with 6 mm diameter of defect size at different depths

4. Experimental Setup

The experiment was carried out in the reflection mode using a focal plane array-based Silver 420 IR camera provided by CEDIP with a spectral range of 3.5 - 5.1µm. The thermography system consists of an indium antimonide semiconductor detector with an internal Stirling cooling system and a spatial resolution of 320 × 256 pixels. The temperature resolution of the camera is 25 mK. In both PT and LT the IR camera and lamps are kept on the same side i.e. in reflection mode (figures 2 & 3). As GFRP material is translucent and more reflective, to increase the emissivity of the test sample solvent removal based black paint was coated on the sample surface.

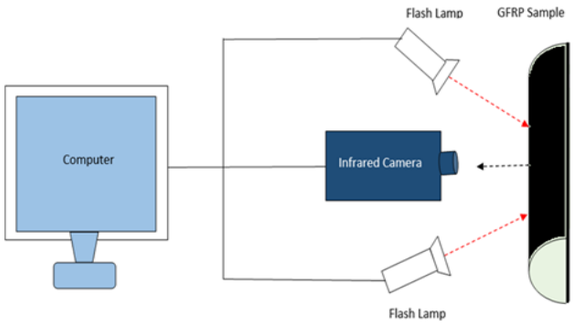

Fig. 2 Schematic diagram of Pulsed Thermography Set Up

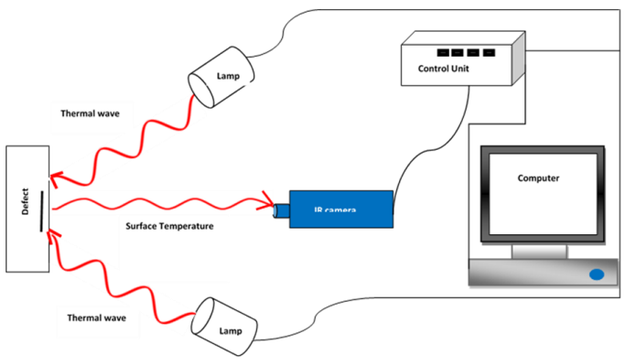

Fig. 3 Schematic diagram of Lock-In Thermography Set Up

4.1 Experimental Setup: Pulsed Thermography

The camera to object distance was kept at 30cm, and the lamp to object distance was kept at 35cm. Two Xenon flash lamps (BALCAR - Nexus 3600 series) with a maximum power of 1600 W and a flash duration of 2 ms were used as the heat source. With maximum deliverable energy at the maximum power (1600 W) is around 4 KJ. The experimental setup is shown in Fig.2. Image sequences were acquired using ALTAIR software, with a 16-bit pseudo color image on display.

4.2 Experimental Setup: Lock-in Thermography

Lock-in thermography was carried out with two halogen lamps as a heat source with a maximum power of 1000 W. Four Point Correlation method proposed by Busse et.al.[1978] is one of the commonly used processing methods for lock-in thermography to get phase, amplitude, and average images that have been adapted for this investigation. The sample was kept close to the IR camera, which covers the maximum area in the 'Field of View' with good spatial resolution. The photograph of the typical experimental setup is shown in Fig. 3.

The frequency selection is carried out based on the defect depth. The defect at 0.6 mm depth (near the surface) is visible at a higher frequency and in the middle range of 0.2–0.05 Hz, defects up to 1.75 mm are visible. At 0.02 Hz frequency, the defects up to 2.85 mm depth are visible, and the 3.5 mm depth of defect is barely visible. At low frequencies (<0.16 Hz) defect depth up to 4.2 mm is visible.

5. Results and Discussion

5.1 Defect Sizing

To analyse the defect size, a 6mm diameter at various depths of 0.6mm, 1.2mm, 1.8mm, 2.4mm, 3.00mm, 3.6mm and 4.2mm is studied with TSR processed PT and LT.

The unprocessed PT and LT thermal images are shown in fig.5 (a & b). Andreas Kromik et al. have studied unidirectional and cross ply laminate composites and analysed the results quantitatively. They have found, the shape of the defects is clearly affected by thermal anisotropy. More importantly, in this analysis, as the sample is curved and due to unidirectional fibre, the defects are appeared as elliptical as shown in fig. 5 (b). In this study, the FWHM method is taken for the measurement of defect size. The size of the defects can be measured by a line profile drawn over the defective area, which is a Gaussian distribution of temperature. A line profile is drawn over the defective region to quantify the defect size. To normalize, a line profile was drawn over the adjacent defect-free region and it was subtracted from the line profile obtained from the defect region.

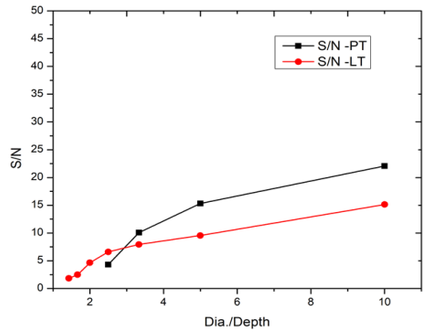

Fig. 4 The diameter-depth ratio versus S/N for PT and LT for each defect

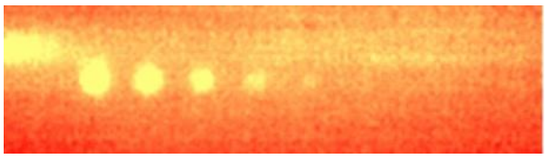

a) Unprocessed Pulsed thermography image

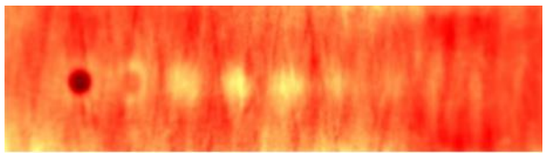

b) Lock In Thermography image

Fig. 5 Thermography images

5.1.1 TSR processed pulsed thermography

From the unprocessed PT thermal image of fig. 5a, the defect up to a depth of 2.4 mm is visible clearly. And the defects above 2.4 mm depth are not visible due to insufficient thermal energy reflection and less signal-to-noise ratio. The measured signal-to-noise value of PT thermal image for depths of 0.6mm, 1.2mm, 1.8mm and 2.4mm are given in table 2. Signal is from defective area and noise is from the non-defective area. These signal's profiles are measured by using Altair software.

S/N= (DS-NDS)/STD (NDS)

Where, DS- Defect signal, NDS- Non defective signal.

To increase the signal-to-noise ratio and increase the defect depth sensitivity, PT thermal images are processed with Thermographic Signal Reconstruction (TSR) which is shown in fig.6 is considered for defect size measurement. The TSR processed image found that the defects which are at higher depth are visible due to noise-free image and increased the depth sensitivity till the depth of 4.2 mm depth is visible as shown in fig. 6. The size of the defects is measured with TSR processed images and found that the maximum depth of 4.2mm of defect is measured with a maximum of -9.17 % error which is presented in table 1.

5.1.2. Lock-in Thermography

In LT, the size of the defects which are close to the surface measured with maximum accuracy with minimum associated error % as reported in table 1. Each defect is measured at its corresponding threshold frequency. The threshold frequencies are considered that at which frequency the particular defect is visible clearly. While increasing the depth the associated error percentage of measurement of defect size is increasing drastically. The size of the defect which is at a higher depth of 4.2 mm is measured with a maximum of 50.83% (table 1). This is due to the GFRP composite's fibre orientation being clearly visible in LT due to the depth of penetration depends on the frequency selection, hence it gives a clear image of fibre orientation, and the same affects the test result also (Fig. 5 b). The LT phase image and the corresponding signal-to-noise ratio are reduced as presented in table 2 and the associated plot is shown in fig.4. In fig.4, the S/N reduces for the decreasing ratio of diameter-depth in PT and LT images. Among PT and LT results, S/N of LT is poor for higher depths as shown in fig. 4. The measured signal-to-noise ratio for various depths of 0.6mm, 1.2mm, 1.8mm, 2.4mm, 3mm, 3.6mm, and 4.2mm is plotted and the linear fit R^2 value is 0.90 as shown in fig. (7) and the values are presented in the table 2.

Table 1 Measured defect size in TSR Processed and Lock-in thermography results

AR	Actual Defect Size (mm)	Defect Depth (mm)	Measured Defect size (mm)				
			Defect size in TSR processed image	Error %	Defect size in LT phase image	Error %	TSR error %
10.00	6	0.6	6.05	-0.83	6.04	0.67	0.83
5.00	6	1.2	6.10	-1.67	6.06	1.00	1.67
3.33	6	1.8	6.15	-2.50	6.40	6.67	2.50
2.50	6	2.4	6.20	-3.33	6.84	14.00	3.33
2.00	6	3.0	6.35	-5.83	7.98	33.00	5.83
1.67	6	3.6	6.42	-7.00	8.55	42.50	7.00
1.43	6	4.2	6.55	-9.17	9.05	50.83	9.17

Table 2 Signal to noise ratio for PT and LT

Defect Size (mm)	Defect depth (mm)	Signal to noise ratio	
		Unprocessed PT	LT
6	0.6	22.05	15.13
6	1.2	15.33	9.55
6	1.8	10.08	7.94
6	2.4	4.30	6.59
6	3.0	-	4.64
6	3.6	-	2.49
6	4.2	-	1.83

5.1.3. Aspect Ratio

Defect depth varies but the same diameter can be analysed by aspect ratio in thermography [Maria Frendberg Beemer et al. 2017]. In an unprocessed thermography image, the Aspect Ratio (AR) threshold is

2 and the deepest defect's AR is less than 2 AR. In LT the defects AR >3 are able to measure with high accuracy (Table 1). AR of TSR processed image is effective for the entire range.

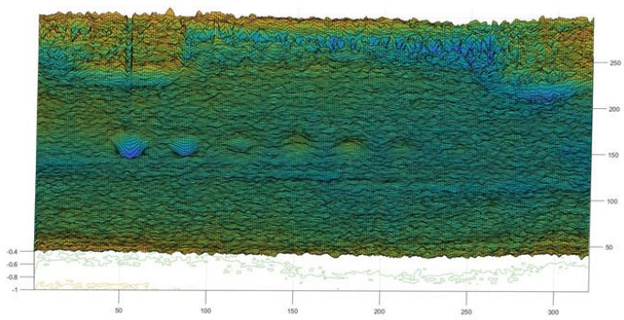

Fig. 6 TSR Processed first derivative PT thermal image at 20 s

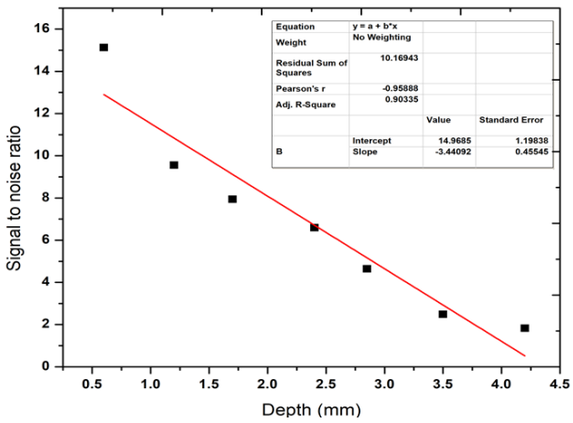

Fig. 7 Signal to noise ratio for various depths in Lock-in thermography

6. Conclusion

The measurement of defect size accuracy is high in TSR processed images of GFRP pipe to the maximum depth of 4.2mm is measured with a maximum of -9.17 % error. Whereas, the measurement of defect size accuracy is very poor for defects that are at higher depth in LT phase images. The maximum depth of 4.2 mm is measured with a maximum of 50.83 % error. This is due to the phase image being affected by fiber orientation (Anisotropy) and the associated signal-to-noise ratio is very poor. This is due to the GFRP composite's fiber orientation being clearly visible in LT because the depth penetration is based on the frequency selection, hence it gives a clear image of fiber orientation and the same affect the test result also.

All the defects which are at different depths are evaluated within a few minutes in TSR processing but in LT, each and every defect's depth has to be evaluated separately. The time taken to evaluate the defects at higher depth by using low frequency will be more in LT. Moreover, multiple acquisitions are required for different frequencies. Hence LT evaluation process is more time- consuming than the processed TSR result.

The size of all simulated defects with a diameter of 6mm and depths ranging from 0.6 to 4.2 mm (Aspect Ratios 1.43 – 10) with less than 10% error using TSR Processed (Fig. 6). For LT, only defects with AR > 3 are measured with error < 10%. LT sizing error approached 50% for defects with AR < 3.

Hence for defect size quantification, the TSR-processed thermal results are recommended and the near-surface defects can be sized with high accuracy in LT. As LT is a time-consuming process for higher depth defects than TSR processed results, impractical in many applications.

Acknowledgements

The authors thank the Director, Indira Gandhi Center for Atomic Research, Kalpakkam for permitting to use the pulse and lock-in thermography facility. This research has not received a specific scholarship from any funding agency.

References

1. *Ahmed Arabi Hassen, U. K.Vaidya, and F. Britt, Structural Integrity of Fiber Reinforced Plastic Piping. Materials Evaluation, Vol. 73. 2015. 918-929. https://www.researchgate.net/publication/281068198_Structural_Integrity_of_Fiber_Reinforced_ Plastic_Piping*

2. *Bates D, Smith G, Lu D, Hewitt J. Rapid thermal non-destructive testing of aircraft components. Composite Part B 2000;31(3):175–85. https://doi.org/10.1016/S1359-8368(00)00005-6*

3. *Julien R. Fleuret , Samira Ebrahimi , Clemente Ibarra-Castanedo and Xavier P. V. Maldague, Independent Component Analysis Applied on Pulsed Thermographic Data for Carbon Fiber Reinforced Plastic Inspection: A Comparative Study, Appl. Sci. 2021, 11, 4377. https://doi.org/10.3390/app11104377*

4. *Yoonjae Chung , Ranjit Shrestha , Seungju Lee and Wontae Kim, Thermographic Inspection of Internal Defects in Steel Structures: Analysis of Signal Processing Techniques in Pulsed Thermography, Sensors 2020, 20, 6015; doi:10.3390/s20216015*

5. *Montanini, R., Freni, F.: Non-destructive evaluation of thick glass fiber-reinforced composites by means of optically excited lock-in thermography. Compos. A 43, 2075–2082 (2012). https://doi.org/ 10.1016/j.compositesa.2012.06.004.*

6. *Sharath, D., Menaka, M., Venkatraman, B.: Defect characterization using pulsed and lock-in thermography: a comparative study. J. Non-destruct. Test. Eval. 32, 134–141 (2012)*

7. *R. Gomathi, M. Ashok, M. Menaka, B. Venkatraman, Quantification of Wall Loss Defect in Glass Fiber Reinforced Polymer Curved Composites Using Lock-In Thermography, Journal of Nondestructive Evaluation volume 40, Article number: 42 (2021).*

8. *Vijayaraghavan, G.K., Sundaravalli, S.: Evaluation of pits in GRP composite pipes by thermal NDT technique. J. Reinfor. Plastics Compos 30, 1599–1604 (2011). https://doi.org/10.1177/07316 84411423119*

9. *Saintey, M.B., Almond, D.P.: Defect sizing by transient thermography. II. A numerical treatment. J. Phys. D Appl. Phys 28, 2539–2546 (1995). https://doi.org/10.1088/0022-3727/28/12/023*

10. *S. G. Pickering & D. P. Almond, An evaluation of the performance of an uncooled microbolometer array infrared camera for transient thermography NDE, Nondestructive Testing and Evaluation, Vol. 22, Nos. 2–3, June–September 2007, 63–70.*

11. *Simon Pickering, Darry Almond, Matched excitation energy comparison of the pulse and lock-in thermography NDE technique, NDT&E International 41 (2008) 501-509.*

12. *Krishnendu Chatterjee, Suneet Tuli, Simon G. Pickering, Darryl P. Almond, A comparison of the pulsed, lock-in and frequency modulated thermography nondestructive evaluation techniques, NDT&E International 44 (2011) 655-667.*

13. *R. Gomathi, M. Ashok, M. Menaka, B. Venkatraman, Characterization of Wall-Loss Defects in Curved GFRP Composites Using Pulsed Thermography, Materials Evaluation (2022), Volume 80, Issue 3.*

14. *S Quek and D P Almond, Defect detection capability of pulsed transient thermography. Insight,Vol 47, No 4, April 2005. https://doi.org/10.1784/insi.47.4.212.63153*

15. *Andrzej Katunin, Krzysztof Dragan, Michał Dziendzikowski, Damage identification in aircraft composite structures: A case study using various non-destructive testing techniques, Composite structures, Vol 127, Sep 2015, Pg 1-9.*

16. *Montanini, R. and F.Freni, Non-destructive evaluation of thick glass fiber-reinforced composites by means of optically excited lock-in thermography, Composites Part A: Applied Science and Manufacturing, 2012. 43(11): p.2075-2082. https://doi.org/10.1016/j.compositesa.2012.06.004*

17. *Wysocka-Fotek, O., M. Maj, and W. Oliferuk, Use Of Pulsed IR Thermography For Determination Of Size And Depth Of Subsurface Defect Taking Into Account The Shape Of Its Cross-Section Area, Archives of metallurgy and materials, Vol. 60. 2015. 10.1515/amm-2015- 0181*

18. *Ranjit, S., Choi, M., Kim, W.: Quantifcation of defects depth in glass fber reinforced plastic plate by infrared lock-in thermography. Journal of Mechanical Science and Technology, 30, 1111–1118 (2016). https://doi.org/ 10.1007/s12206-016-0215-5.*

19. *Sakagami, T., Kubo, S.: Applications of pulse heating thermography and lock-in thermography to quantitative nodestructive evaluations. Infrared Physics and Technology, 43, 211–218 (2002). https:// doi.org/10.1016/S1350-4495(02)00141-X*

20. *G. Busse, P. Eyerer, Thermal wave remote and nondestructive inspection of polymers, Applied Physics Letters, 43 (1983) 355-357. https://doi.org/10.1063/1.94335.*

21. *Olga Wysocka-Fotek , Wiera Oliferuk, Michał Maj. Reconstruction of size and depth of simulated defects in austenitic steel plate using pulsed infrared thermography. Infrared Physics & Technology, 55 (2012), 363-367. DOI:10.1016/j.infrared.2012.02.004.*

22. *G. Busse, Photothermal transmission probing of a metal, Infrared Physics, 20 (1980) 419-422.*

23. *Andreas Kromik, Zia Javanbakht, Brenton Miller, Ian Underhill, Wayne Hall, On the Effects of Anisotropy in Detecting Flaws of Fibre-Reinforced Composites, Applied Composite Materials, 2022. https://doi.org/10.1007/s10443-022-10067-8*

24. *Maria Frendberg Beemer & Steven M. Shepard, Aspect ratio considerations for flat bottom hole defects in active thermography, Quantitative InfraRed Thermography Journal, 2017. doi:10.1080/17686733.2017.1328642*

25. *Milne JM, Reynolds WN. The non-destructive evaluation of composites and other materials by thermal pulse video thermography. Proc Soc Photo-Opt Instrum Eng 1985:119–22.*

26. *Lau SK, Almond DP, Milne JM. A quantitative analysis of pulsed video thermography. Non-Dest Test Eval Int 1991;24:195–202.*

27. *Shepard S. Advances in pulsed thermography. In: Rozlosnik AE, Dinwiddie RB, editors. Thermosense XIV, SPIE proceedings, vol. 4360; 2001. p. 511–5.*

28. *Busse G, Wu D, Karpen W. Thermal wave imaging with phase sensitive modulated thermography. J Appl Phys 1992;71(8):3962–5.*

29. *Busse G. Optoacoustic phase angle measurement for probing a metal. Appl Phys Lett 1979;35:759–60*

30. *Shepard SM. Temporal noise reduction, compression and analysis of thermographic image data sequences. US Patent 6516084. 2003.*

31. *Daniel Balageas, Bastien Chapuis, Geoffrey Deban & Françoise Passilly, Improvement of the detection of defects by pulse thermography thanks to the TSR approach in the case of a smart composite repair patch, Quantitative InfraRed Thermography Journal, 2012, 167-187.*

32. *S.M. Shepard, J.R. Lhota, B.A. Rubadeux, T. Ahmed and D. Wang, Enhancement and reconstruction of thermographic NDT data, Proceedings of SPIE Vol. 4710 (2002).*